

Cite this: *Chem. Commun.*, 2011, **47**, 5199–5201

www.rsc.org/chemcomm

An organometallic derivative of a BAPTA ligand: towards electrochemically controlled cation release in biocompatible media†

Koyel X. Bhattacharyya,^a Leïla Boubekeur-Lecaque,^a Issa Tapsoba,^a Emmanuel Maisonhaute,^{ab} Bernd Schöllhorn^{ac} and Christian Amatore^{*a}

Received 23rd February 2011, Accepted 8th March 2011

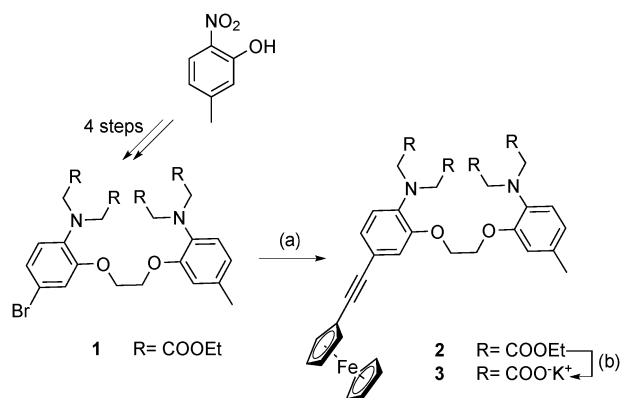
DOI: 10.1039/c1cc11081k

The combination of a ferrocenyl moiety with BAPTA provides a novel, water-soluble, redox-active chelator. This chelator behaving as a conformational sensor exhibits an unexpected electrochemical response with high affinity and selectivity for calcium.

Calcium behaves as a chemical messenger in a wide variety of cells, and local variations in its concentration play a key role in many biological processes.^{1,2} The understanding of how calcium affects cellular functions necessitates the precise modulation of calcium concentration with high spatial and temporal resolution. Tremendous efforts have led to the development of molecules designed to encapsulate calcium, and more importantly, to capture and release calcium under external physicochemical stimuli such as photons. The design of such molecules must fulfill strict requirements dictated by biological constraints (water solubility, physiological pH, remarkable selectivity for calcium over all other competing cations, and biological inertness). Tsien's group has developed and thoroughly studied a series of calcium chelators based on BAPTA (1,2-bis(*o*-aminophenoxy)ethane-*N,N,N',N'*-tetraacetic acid)-type ligands, which coordinate Ca²⁺ with high affinity and sufficient selectivity over the most likely competing ions, such as Na⁺, K⁺, and Mg²⁺.³ This family of molecules opened new possibilities of Ca²⁺ study, such as calcium buffering and mapping inside cells or the triggering of calcium release/uptake using light as an external command.⁴ Although it is a very powerful approach, the main drawback of the photo-induced calcium release remains the irreversibility since the chelation ability is definitively lost upon photolysis. Alternatively, electrochemistry is an attractive approach to reversibly switch the cation affinity. Moreover the peculiar properties of diffusion at ultramicroelectrodes would *a priori* allow the cation release with high spatial and temporal resolution. The use of electrochemistry to probe cation affinity is not

unprecedented in the literature, though it is typically seen in the framework of sensor applications and is conducted in organic solvents.⁵ Recently, our group has demonstrated that caged calcium in redox-active aza-crown ethers is released in organic solvents with high spatial and temporal resolution using electrons as an external stimulus.⁶ However, this system proved to be ineffective in water, preventing studies in biological media. In order to overcome this drawback, we envisioned the union of BAPTA with the redox properties of ferrocene to design a new water-soluble, redox-active ligand with high affinity and excellent selectivity towards calcium. The efficient interplay between the binding and the redox subunits is based on through bond communication *via* an ethynyle linker. Herein we describe the design, synthesis, and characterization of a new organometallic chelator aimed at developing an electrochemical approach for the selective capture and release of calcium ions under physiological conditions.

Among the large variety of BAPTA derivatives described in the literature,^{1,7} bromo-substituted BAPTA has been selected as a building block for the synthesis. The mono-halogenated arene **1** reported by Gryniewicz *et al.* was conveniently used to form C–C bonds by palladium catalyzed coupling reactions.⁸ The synthesis of the novel organometallic derivative **3** was carried out in six steps from 2-nitrophenol and 2-nitro-5-methylphenol (see Scheme 1 and the ESI†). Sonogashira coupling of derivative **1** with ethynylferrocene provided the desired proligand **2** in 38% yield, which is satisfactory



Scheme 1 Synthesis of Ligand **3**: (a) PdCl₂(PPh₃)₂, ethynylferrocene, DMF, iPr₂NH, 110 °C (38%); (b) KOH, THF/water (>98%)

^a Department of Chemistry, UMR 8640 CNRS-ENS-UPMC, Ecole Normale Supérieure, 24 rue Lhomond, 75005 Paris, France. E-mail: christian.amatore@ens.fr; Fax: +33 1-44323863

^b Laboratoire Interfaces et Systèmes Electrochimiques-UPR 15, Université Pierre et Marie Curie-Paris 06, 75005 Paris, France

^c Laboratoire d'Electrochimie Moléculaire, Université Paris Diderot, UMR CNRS 7591, 15 rue Jean de Baïf, 75013 Paris, France

† Electronic supplementary information (ESI) available: Experimental details for the synthesis, UV-Vis and electrochemical studies. See DOI: 10.1039/c1cc11081k

considering the highly deactivated nature of the bromoarene. Subsequent alkaline hydrolysis of the tetrakis ester **2** yielded the corresponding tetrapotassium salt **3**.

UV-Visible spectroscopy (UV-Vis) and cyclic voltammetry (CV) studies were conducted in buffered aqueous solutions to evaluate the calcium affinity of ligand **3** and to investigate redox-induced cation release. In the absence of calcium, chelator **3** mainly exhibits two absorption maxima at 319 nm ($\epsilon = 3.10 \times 10^4 \text{ M}^{-1} \text{ cm}^{-1}$) and 430 nm ($\epsilon = 2.10 \times 10^3 \text{ M}^{-1} \text{ cm}^{-1}$). The large absorbance band in the 270–380 nm range shifts to shorter wavelengths upon calcium binding. Conversely, the weaker band around 430 nm is barely affected by the increase in the calcium concentration.

Changes in UV-Vis spectra upon complexation (Fig. 1) provide the stoichiometry of complexation and its affinity constant. For this purpose, the absorbance values at two different wavelengths (266 and 326 nm) for various free calcium concentrations set by EGTA buffer have been processed in Hill plots. The linear behavior with an absolute value of the slope equal to 1 is fully consistent with the expected 1 : 1 complex of calcium (see inset, Fig. 1). Furthermore, identical x -axis intercepts for the two selected wavelengths allow us to estimate a dissociation constant K_d^{Ca} of $320 \pm 8 \text{ nM}$ (at $22 \pm 2 \text{ }^\circ\text{C}$, $\text{pH} = 7.2$) for ligand **3**. A similar study conducted with magnesium showed that the UV-Vis properties of **3** require a millimolar scale concentration of Mg^{2+} to be significantly perturbed ($K_d^{\text{Mg}} = 6.0 \pm 0.5 \text{ mM}$ at $20 \pm 2 \text{ }^\circ\text{C}$; details given in the ESI†). The values of the dissociation constants determined for Ca^{2+} and Mg^{2+} differ by four orders of magnitude, ensuring that chelator **3** is able to discriminate between the cation of interest, namely, Ca^{2+} , and its serious competitors, such as Mg^{2+} , that are present in biological media at much higher concentrations.

The electrochemical behavior of free ligand **3** is characterized by a first reversible process at 205 mV vs. SCE involving the iron center, and a second irreversible process at 495 mV from the oxidation of the amino groups on the benzene rings.

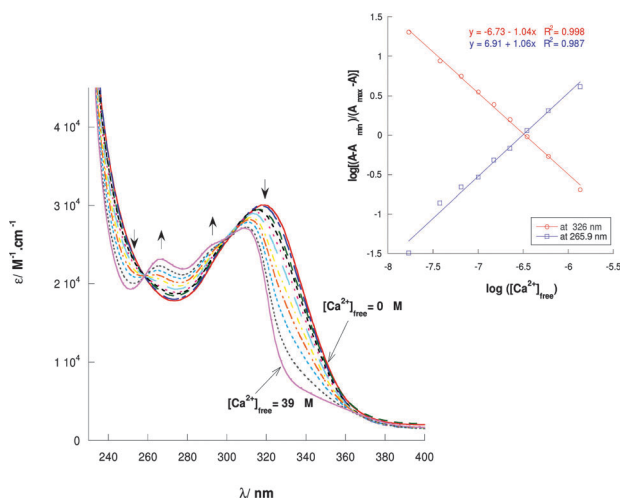


Fig. 1 UV-Vis absorption spectra of **3** for different free Ca^{2+} concentrations set by EGTA buffer (0.1 M KCl, 30 mM MOPS $\text{pH} = 7.2$, 10 mM EGTA). Inset: Hill plot for absorbance at 266 and 326 nm. A_{min} (A_{max}) is the absorbance of the free ligand **3** (Ca^{2+} complex, respectively).

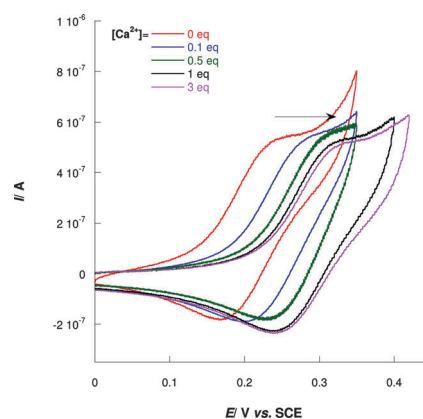


Fig. 2 Effect of Ca^{2+} concentration on the electrochemical response of **3** (1 mM) in aqueous solutions (0.1 M KCl, 30 mM MOPS $\text{pH} = 7.4$). Scan rate: 100 mV s^{-1} on a glassy carbon electrode.

A gradual increase in Ca^{2+} concentration leads to an anodic potential shift of the Fc/Fc^+ redox couple, but does not affect the reversible shape of the peak (Fig. 2). The magnitude of the potential shift reaches 80 mV for 1 equivalent of Ca^{2+} per ligand. Further increases in Ca^{2+} concentration or the addition of a large excess of Mg^{2+} have no significant effect on the oxidation peak potential, which is fully consistent with a 1 : 1 stoichiometry, as evidenced by UV-Vis.

However, our results differ widely from the predictions based on the square scheme mechanism often relevant for such chelators with high affinity constants. In this framework, two limiting electrochemical behaviors (“two-wave” vs. “anodic shift”) are described in the literature in the presence of sub-stoichiometric amounts of cations.^{9,10} According to this commonly accepted reversible square scheme mechanism (see ESI†), the dissociation constant would be predicted in our case to be $K_d^{\text{theo}}(\text{OX}) \approx 24 \cdot K_d^{\text{Ca}} \approx 7.7 \text{ } \mu\text{M}$ for the oxidized form of the chelator 3^+ .¹¹ This predicted value was compared to the affinity constant obtained experimentally by UV-Vis for the chemically oxidized chelator $K_d^{\text{exp}}(\text{OX}) = 460 \pm 35 \text{ nM}$. The discrepancy between these values led us to test the validity of the reversible square scheme in our case. Digital CV simulations of the square scheme mechanism based upon the set of parameters obtained

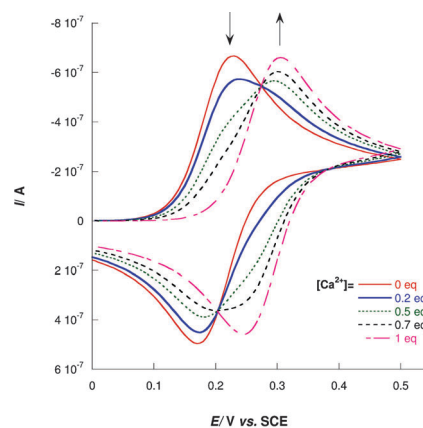


Fig. 3 Simulated CV of ligand **3** ($E^{\text{O}'} = 0.2 \text{ V}$ for the free ligand, $E^{\text{O}'} = 0.28 \text{ V}$ for the complex) with different amounts of Ca^{2+} . $[\text{Ligand } \mathbf{3}] = 1.0 \text{ mM}$, scan rate = 100 mV s^{-1} , $K_{\text{red}} = 3.10 \times 10^6 \text{ M} = 1/K_d^{\text{Ca}}(\text{RED})$.

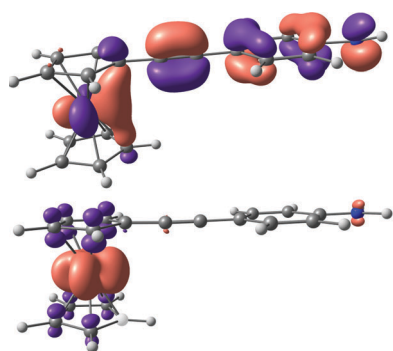


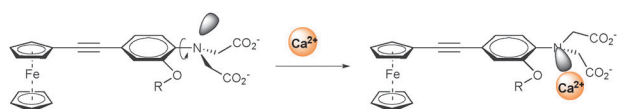
Fig. 4 HOMO orbital (top) and spin-density isosurface (bottom) of the oxidized form of the model system. Contour values are plotted at ± 0.04 ($e \text{ bohr}^{-3}$)^{1/2} for molecular orbitals and at ± 0.003 a.u. for spin density.

experimentally clearly show (Fig. 3) that even for our rather small potential separation, a two-wave behavior should be observed, such that two separate redox signals (free and complexed ligands) appear at potentials that are independent of cation concentration. Therefore, a more complex mechanism coupling complexation to electron transfer governs the unexpected anodic shift behavior of our system.

The measured affinity for the oxidized form seeming barely affected by the oxidation prompted us to reexamine the mutual influence between Ca^{2+} and the ferrocenyl moiety. Indeed the effective electronic communication between the redox and the coordinating subunits of the ligand is a stringent requirement to observe a significant cation affinity modulation.⁹ On the molecular level, DFT calculations were carried out on model systems of the free ligand and the calcium complex, to examine whether the oxidation of ligand **3** significantly impacts the cation binding.

The long-range electronic communication between the iron and the nitrogen atom implies that the removal of one electron (oxidation process) from the HOMO (Fig. 4) should affect the chelation ability of the nitrogen atom. The spin density of the oxidized ligand (Fig. 4) reveals a non-negligible contribution of the nitrogen atom, though the iron center carries the largest positive spin density. Thus, this simplified electronic structure calculation confirms that the oxidation of the iron centre is associated with a weakening of the donating ability of the nitrogen atom towards the coordinated cation (Ca^{2+} , etc.).

The interaction of Ca^{2+} with the BAPTA ligand in the gas phase reveals structural distortions from planarity with rotation around the C(aryl)–N bond as required for the coordination of Ca^{2+} (Scheme 2).¹² Whether this structural reorganization is concerted or sequential cannot be decided presently. However in either case these results strongly support the inadequacy of simple square scheme formulation. Along with the conformational change, the nitrogen lone pair is no longer involved in the



Scheme 2 Structural distortion upon complexation of Ca^{2+} .

π system of the phenyl ring, but instead takes part in calcium binding. Therefore, the anodic shift of the ferrocenyl redox response is not directly linked to the decrease of electronic density on the nitrogen atom upon coordination of Ca^{2+} , but is more likely due to the rotation of the amino substituent with respect to the phenyl plane. In the complexed ligand, the electron donating amino group is much less involved in the molecular conjugation, leading to a decrease in electronic density in the phenyl π system, and thus *a fortiori* on the remote ferrocenyl group.

In conclusion, a novel, water-soluble, redox-active, and selective calcium chelator was designed. Joint theoretical and experimental studies reveal unexpected electrochemical behavior for this chelator with high affinity for Ca^{2+} , behaving as a conformational sensor. Work is thus currently underway to explore other synthetic approaches which may lead to a larger cationic charge localization within the chelating moiety of the ligand.¹³

This work was supported by the CNRS (UMR 8640 and LIA XiamENS), ENS, the Université Pierre et Marie Curie, the ANR through REEL Blan06-2_136291 and the Franco-American Commission through the Fulbright advanced student fellowship (KXB).

Notes and references

- G. C. R. Ellis-Davies, *Chem. Rev.*, 2008, **108**, 1603–1613.
- R. Y. Tsien, Fluorescent Chemosensors for Ion and Molecule Recognition, *ACS Symp. Ser.*, 1993, **538**, 130–146.
- R. Y. Tsien, *Biochemistry*, 1980, **19**, 2396–2404.
- S. R. Adams, J. P. Y. Kao, G. Gryniewicz, A. Minta and R. Y. Tsien, *J. Am. Chem. Soc.*, 1988, **110**, 3212–3220; S. R. Adams, J. P. Y. Kao and R. Y. Tsien, *J. Am. Chem. Soc.*, 1989, **111**, 7957–7968.
- P. D. Beer, P. A. Gale and G. Z. Chen, *Coord. Chem. Rev.*, 1999, **186**, 3–36; P. D. Beer, P. A. Gale and G. Z. Chen, *J. Chem. Soc., Dalton Trans.*, 1999, 1897–1909; P. D. Beer, C. Blackburn, J. F. McAleer and H. Sikanyika, *Inorg. Chem.*, 1990, **29**, 378–381; H. Plenio and D. Burth, *Organometallics*, 1996, **15**, 4054–4062; H. Plenio, D. Burth and R. Vogler, *Chem. Ber.*, 1997, **130**, 1405–1409.
- C. Amatore, D. Genovese, E. Maisonhaute, N. Raouafi and B. Schöllhorn, *Angew. Chem., Int. Ed.*, 2008, **47**, 5211–5214.
- P. S. Mohan, C. S. Lim, Y. S. Tian, W. Y. Roh, J. H. Lee and B. R. Cho, *Chem. Commun.*, 2009, 5365–5367; R. Pethig, M. Kuhn, R. Payne, E. Adler, T. H. Chen and L. F. Jaffe, *Cell Calcium*, 1989, **10**, 491–498; X. H. Dong, Y. Y. Yang, J. Sun, Z. H. Liu and B. F. Liu, *Chem. Commun.*, 2009, 3883–3885.
- G. Gryniewicz, M. Poenie and R. Y. Tsien, *J. Biol. Chem.*, 1985, **260**, 3440–3450.
- A. E. Kaifer and S. Mendoza, in *Comprehensive Supramolecular Chemistry*, ed. G. W. Gokel, Elsevier, New York, 1996, vol. 1, pp. 701–731.
- A. E. Kaifer, *Acc. Chem. Res.*, 1999, **32**, 62–71.
- In square schemes, the voltammetric behavior is governed by the equilibrium constants K_{red} and K_{ox} corresponding to the complexation of Ca^{2+} by the reduced (**3**) and oxidized (**3⁺**) forms of the ligand and related by: $\ln\left(\frac{K_{\text{ox}}}{K_{\text{red}}}\right) = \frac{nF}{RT}(E_{\text{ligand}}^{\text{O}'} - E_{\text{complex}}^{\text{O}'})$, $E_{\text{ligand}}^{\text{O}'}$ and $E_{\text{complex}}^{\text{O}'}$ being the formal potentials for the oxidation of the free ligand and complex. n is the number of electrons involved in the redox process (here equal to 1).
- J. T. Gerig, P. Singh, L. A. Levy and R. E. London, *J. Inorg. Biochem.*, 1987, **31**, 113–121; C. K. Schauer and O. P. Anderson, *J. Am. Chem. Soc.*, 1987, **109**, 3646–3656.
- The screened positive charge created on the ferrocenyl appears to have a low influence on the electrostatic repulsion force on the Ca^{2+} in agreement with the use of Fc^+/Fc as a reference redox couple.